

Structure and Stability of Non-Transform Discontinuities on the Mid-Atlantic Ridge between 24° N and 30° N

SARA SPENCER¹, DEBORAH K. SMITH², JOHNSON R. CANN³, JIAN LIN² and EDWARD McALLISTER³

¹ *Department of Geology, American University of Beirut, Beirut, Lebanon*

² *Department of Geology and Geophysics, Woods Hole Oceanographic Institution, Woods Hole, MA 02543, U.S.A.*

³ *Department of Earth Sciences, University of Leeds, Leeds, LS2 9JT, U.K.*

(Received 6 August 1996; accepted 27 June 1997)

Key words: Non-transform discontinuities, Mid-Atlantic Ridge, spreading segments, side-scan sonar, septa, brittle/ductile shear, non-tectonised offsets

Abstract. Observations of the median valley within the 24–30° N area of the Mid-Atlantic Ridge (MAR), using the IOSDL high resolution side-scan sonar instrument TOBI, image four separate areas of the median valley, containing part or all of nine spreading segments, and five non-transform discontinuities between spreading segments (NTDs). These high resolution side scan images were interpreted in parallel with multibeam bathymetry (Purdy et al., 1990), giving a greater degree of structural precision than is possible with the multibeam data alone. Three distinct types of NTD were identified, corresponding in part to types previously identified from the multibeam bathymetric survey of the area. Type 1 NTDs are termed septal offsets, and are marked by a topographic ridge separating the two spreading segments. The offset between the spreading segments ranges from 9 to 14 km. These can be further subdivided into Type 1A in which the septa run parallel to the overall trend of the MAR and Type 1B in which the septa lie at a high angle to the bulk ridge trend. Type 1A NTDs are characterised by overlap of the neovolcanic zones of the segments on each side, and strong offaxis traces, while Type 1B NTDs show no overlap of neovolcanic zones, and weak offaxis traces. Type 2 NTDs are brittle/ductile extensional shear zones, marked by oblique extensional fractures, and associated with rotation of tectonic and volcanic structures away from the overall trend of the MAR. Type 3 NTDs are associated with offsets of less than 5 km, and show no sign of any accommodating structure. In this type of NTD, the offset zone is covered with undeformed volcanics. The type of NTD developed at any locality along the ridge axis appears to depend on the amount of segment offset and segment overlap, the overall trend of the mid-ocean ridge, the width of the zone of discontinuity, the median valley offset and the longevity of the offset. These factors influence the mechanical properties of the lithosphere across the discontinuity, and ultimately the tectonic style of the NTD that can be supported. Thus brittle/ductile extensional shear zones are long-lived structures favoured by large segment offsets, and small or negative segment overlaps. Septa can be short or long lived, and are associated with large segment offsets. Segment overlaps vary from negative (an along axis gap) to zero, for Type 1B septal offsets, or positive to zero for Type 1A septal offsets. Non-tectonised NTDs are generally short lived structures, characterised by small segment offsets and zero or positive overlaps.

Introduction

It has long been recognised that the Mid-Atlantic Ridge is divided into distinct accretionary segments which are oriented at right angles to the spreading direction and which are offset from one another by axial discontinuities (e.g. Johnson and Vogt, 1973; Rona, 1976; Searle and Laughton, 1977; Phillips and Flemming, 1977; Ramberg et al., 1977; Rona and Gray, 1980; Schouten et al., 1985; Brozena and Chayes, 1988; Macdonald et al., 1988; Sempéré et al., 1990, 1993; Fox et al., 1991; Grindlay et al., 1991; Carbotte et al., 1991). Offsets on slow-spreading ridges have previously been classified using bathymetric morphology, with particular emphasis on the size of the offset between adjacent segments, their longevity and the orientation of their off-axis traces relative to the spreading axis (Rona, 1976; Rona and Gray, 1980; Macdonald et al., 1988; Grindlay et al., 1991; Sempéré et al., 1993). Rona and Gray (1980) distinguished two classes of offset, which they referred to as major and minor fracture zones. Major fracture zones were defined as linear, well-defined offsets of greater than 50 km (crustal age offsets of 2–3 Ma) in which the off-axis trace is symmetrical with respect to the spreading axis and coincides with small circles about the pole of plate rotation (Searle, 1986; Tamsett and Searle, 1988). Major fracture zones are thus transform faults *sensu stricto*, which in the Mid-Atlantic cut across the ridge at 200–800 km intervals (Fox and Gallo, 1986) and include the Kane and Atlantis fracture zones. Rona and Gray's minor fracture zones are associated with a much shorter offset, generally less than 30 km, which cross-cut the ridge at intervals of less than 80 km (Schouten et al., 1985; Macdonald, 1986; Macdonald et al., 1988). The off-axis traces of minor fracture zones are not parallel to the small circles about the poles of plate rotation (Rona and Gray, 1980). More recently, con-

tinuous high-resolution multibeam bathymetric mapping of two areas of the Mid-Atlantic Ridge (Purdy et al., 1990; Fox et al., 1991) has led to a re-definition of the minor fracture zones. Detailed analysis of their morphology has shown that unlike transform faults, the minor fracture zones are not marked by a well-defined, single, linear fault zone valley, but are made up of diffuse zones marked by basins and/or intra-segment highs (Sempéré et al., 1990; 1993; Grindlay et al., 1991). These offsets are referred to as accommodation zones (e.g. Karson, 1990) or non-transform discontinuities (NTDs; e.g. Macdonald et al., 1988; Lonsdale, 1989).

In this paper we examine non-transform discontinuities on the Mid-Atlantic Ridge between 24° and 30° N, using Sea Beam multibeam bathymetric data (Purdy et al., 1990), high resolution deep-towed side scan sonar images (Smith et al., 1995) and satellite free air gravity anomalies (Sandwell and Smith, 1992). Using this data we establish a new classification for NTDs based on their structural style and their relationship to the overall configuration of the ridge axis. In the light of these results we discuss their temporal development.

Previous Classification of Non-Transform Discontinuities

Existing kinematic models of NTDs have been developed at fast- and intermediate-spreading ridges. These include overlapping spreading centres (Macdonald et al., 1984, 1986; Lonsdale, 1986) and propagating rifts (Hey, 1977; Hey et al., 1980; Hey et al., 1986; McKenzie, 1986; Kleinrock and Hey, 1989). Similar models for slow-spreading ridges (Sempéré et al., 1990, 1993; Lin et al., 1990; Grindlay et al., 1991) are still evolving, although descriptions based on gravity and magnetic signature and the broad morphological features provided through the analysis of bathymetric data have allowed a basic classification to be established.

Using this approach, NTDs from both fast- and slow-spreading ridges are subdivided into three categories on the basis of the size of the ridge-ridge offset and their longevity. These categories are second-, third- and fourth-order discontinuities (Macdonald et al., 1988; Grindlay et al., 1991; Sempéré et al., 1993), where first-order discontinuities are transform faults *sensu stricto*. Second-order discontinuities are defined as having ridge-ridge offsets of approximately 15–30 km and a recognisable off-axis trace indicating their continued existence at a given latitude over a 1–3 Ma period (Macdonald et al., 1988). At the slow-spreading

MAR they are characterised by localised rotations of the neo-volcanic zone of up to 10° and along axis depth anomalies of several hundred metres (Sempéré et al., 1993). Sempéré et al. (1993) described these as degenerate transforms, overlapping rift valleys and intra-rift offsets in which the two segments may or may not be separated by an extensional basin. Third-order discontinuities are characterised by a similar ridge-ridge offset but have no recognisable off-axis trace indicating that they are relatively young features (Macdonald et al., 1988; Grindlay et al., 1991). These offsets are marked by along axis depth anomalies of a few hundred metres and localised rotation of the neo-volcanic zone of less than 5° (Sempéré et al., 1993). They have been described by Sempéré et al. (1993) as small scale en echelon jogs with or without an extensional basin between the two offset segments. Finally, fourth-order discontinuities represent offsets within the neo-volcanic zone of less than 4 km. They are commonly associated with small basins (<200 m) and in the absence of a robust axial-volcanic ridge they correspond to gaps between isolated seamounts or strings of seamounts (Sempéré et al., 1993).

Acquisition and Data Analysis

During February 1992 data were collected on Cruise 65 of RRS *Charles Darwin* (CD65) within the median valley of the Mid-Atlantic Ridge (24–30° N; Figure 1) using the high resolution side-scan sonar instrument TOBI. TOBI is a deep-towed vehicle which houses a variety of sensors including a 30–32 kHz dual-sided side-scan sonar (swath width of 6 km), a 7.5 kHz sub-bottom seismic profiler, a triaxial fluxgate magnetometer, a temperature sensor, and a photo-transmissometer (Flewellen et al., 1993). The vehicle was towed at 400–800 m above the ocean floor along a series of closely spaced parallel tracks. This produced a dense mosaic of overlapping images, which covered most of the median valley and allowed dual insonification of many features. Resolution is range dependent; but on average the image pixel size is approximately 10 m. On the images, areas of bright back-scatter represent bare rock surfaces especially where they tilt towards the vehicle, and dark areas are shadows, representing surfaces that dip away from the vehicles track. Individual seamounts are represented by raised circular features (W in Figures 6b and 8b), which are sometimes botryoidal. Fault scarps show up as linear zones of high back scatter (Y in Figure 4b) where they tilt towards the vehicles track and shadow (Z in Figures 4b and 8b) where they tilt away from it. Clastic sediments

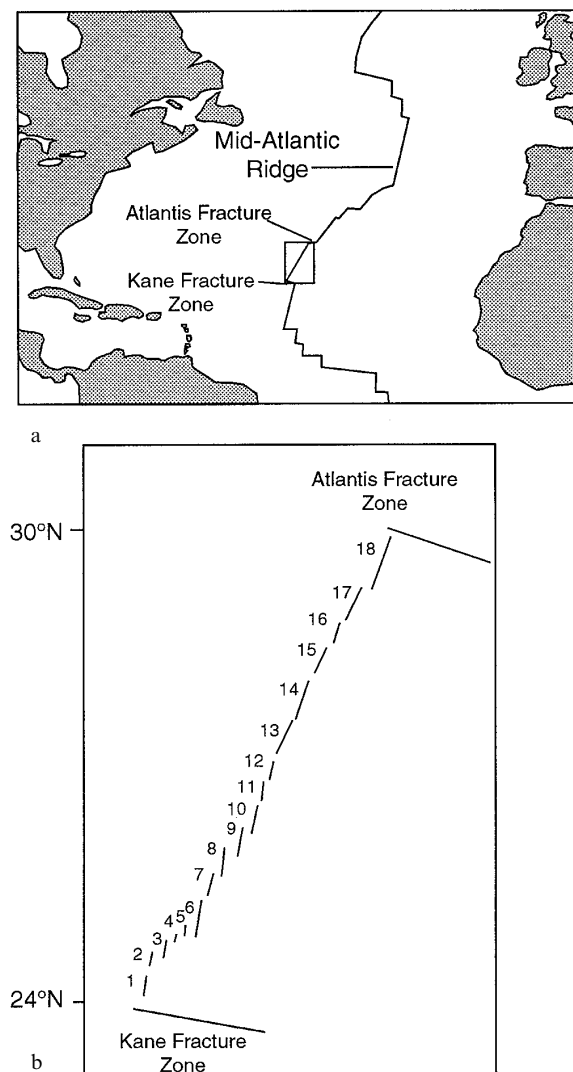


Fig. 1. (a) Location map showing the northern Mid-Atlantic Ridge. The boxed area which includes the Kane and Atlantis fracture zones corresponds to the site of multibeam bathymetry surveys (Purdy et al., 1990). (b) An enlargement of the boxed region showing the axes of the eighteen (1–18) spreading segments as defined from the bathymetry (after Smith et al., 1994).

associated with landslides and debris slopes on fault scarps are associated with the zones of high backscatter, whilst thick pelagic sediments attenuate the signal and are thus characterised by zones of dark grey. All of the side-scan images were manually co-registered with the multibeam bathymetric data of Purdy et al. (1990).

Satellite-free air gravity anomalies for the area were obtained from Sandwell and Smith (1992). Figure 2 shows the free air gravity anomalies as determined

from satellite orbits. Most of the signal at short wavelengths picks up seafloor topography at a scale of kilometres to tens of kilometres. The areal extent of the data and its uniformity makes it useful in determining the off-axis traces of the segments and the inter-segment offsets (Figure 2).

During the CD65 cruise between 24°–30° N four separate areas of the median valley were insonified by TOBI, containing part or all of nine of the eighteen spreading segments and four of the seventeen non-transform discontinuities between the Kane and Atlantis fracture zones (Figure 1b). Using the TOBI images we were able to examine the character of faults (displacement direction, dip of fault blocks) within and adjacent to the discontinuity and to look at their relationship to the volcanic morphology of the spreading segments. Many of the faults that we identified had not been previously recognised in the multibeam bathymetric data, which has a much lower resolution (McAllister and Cann, 1996). Using the TOBI images together with the multibeam bathymetric data (Purdy et al., 1990) we were able to recognise on structural grounds three distinct types of NTD. Table I shows the data that were collected for each offset, using multibeam bathymetry interpreted in the light of the TOBI images. On each side of an offset, the position of the neovolcanic zone in each segment was established from the morphology of the axial volcanic ridge, and the end of each axial volcanic ridge determined by the last occurrence of fresh volcanic features, as indicated by the high resolution back scatter data where they exist. We measured the size of the offset between adjacent spreading axes, the length of the overlap between the neovolcanic zones of adjacent spreading segments (negative values mean that the neovolcanic zones fail to overlap by the stated amount), the size of offset of the median valley (defined by the innermost major faults on the valley wall), the width of the zone of discontinuity (see Figure 3) and its spatial longevity measured as a function of its off-axis bathymetric and gravity traces (Rona, 1976; Rona and Gray, 1980; Sempéré et al., 1993; Sandwell and Smith, 1992).

Types of Non-Transform Discontinuity

In this section we describe the morphology and structural style of the seventeen NTDs between 24°–30° N, based on TOBI imagery of five NTDs and multibeam bathymetry of all seventeen. Of the seventeen, nine have been identified as septal offsets, three as extensional shear zones and five as non-tectonised discontinuities.

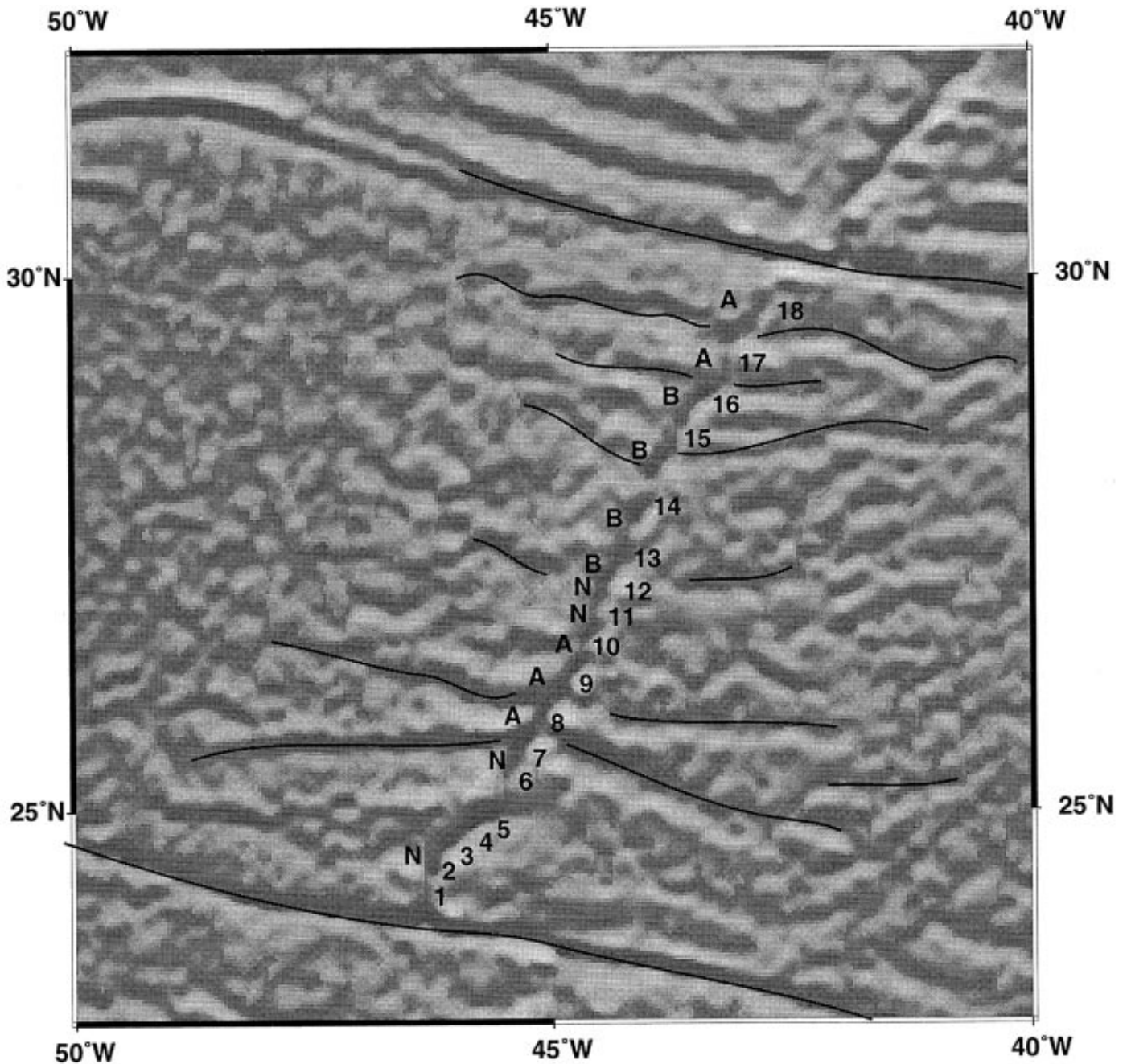


Fig. 2. Gray-scale shaded relief image of satellite gravity data, illustrating the segmented nature of the Mid-Atlantic Ridge, after Sandwell and Smith (1992). Numbers refer to individual spreading segments which are marked by a solid black line. A represents Type A septa, B, Type B septa and N, non-tectonised, non-transform discontinuities. The off-axis traces of persistent NTDs are marked by solid black lines.

TYPE 1: SEPTAL OFFSETS

Septal Offsets at 25°36' N and 28°51' N

Previously identified by Sempéré et al. (1993), the NTD at 25°36' N (Figure 4a-c) has been described as a

second-order discontinuity with a dextral segment offset of 11 km and a discontinuity width of -9 km. This NTD is characterised by a steep-sided ridge between the two offset segment ends, termed here a septal high or septum. The septum separates two segments (seg-

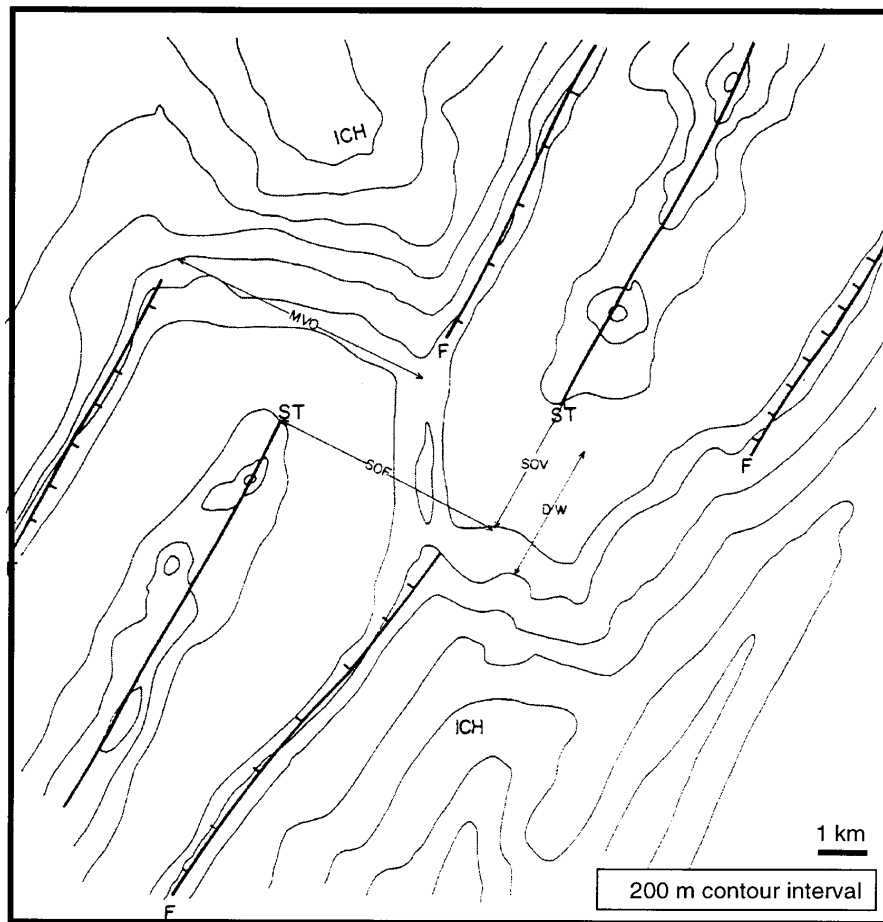


Fig. 3. Schematic representation of the bathymetry data across a NTD showing the spreading axis (solid black line, considered to coincide with the centre of the AVR as determined from their neo-volcanic morphology), the segment terminations (ST), the first median valley faults (F) and the inner corner highs (ICH). The size of the segment offset was determined by measuring the distance in the spreading direction between the axes of two adjacent segments (SOF). The amount of overlap was determined by measuring the distance between the tips of two adjacent segments as determined from their neo-volcanic morphology in a direction parallel to the ridge axis (SOV). Positive values represent an overlap of the segments and negative values represent an along-axis gap. The offset of the median valley was determined by measuring the distance in a direction perpendicular to the ridge axis between the first median valley faults across the discontinuity (MVO). The width of the zone of discontinuity was determined by measuring the distance between the two inner corner highs, as defined by an abrupt change in the orientation of the contours, in a direction parallel to the ridge axis (DW). Positive values represent an overlap of the inner corner highs and negative values represent a gap between the inner corner highs. This measurement could not be determined for all of the NTDs since some lack well-developed inner corner highs.

ments 7 and 8, Figure 2) which overlap by 7.7 km. It comprises a series of linked oval and arcuate highs which trend 340° , linking the inside corner highs which lie at the northern and southern terminations of the segments (Figure 4a). On the side-scan sonar image (Figures 4b–c) these highs are seen to comprise a series of en echelon fault blocks which trend 015° – 020° and step down to the east. The faults bounding these blocks have a similar orientation to those in the adjacent segments (015° – 023° , Escartin and Lin, 1995) and are

considered to be part of the array of faults which form the median valley wall to the west of the northern segment. Similarly oriented faults and fault blocks can also be seen within the segments, where they dissect the ends of the axial volcanic ridges (Figures 4b–c). The faults in both segments and across the septum do not appear to be isolated structures but rather form part of an array of dominantly easterly downthrowing faults which cross-cut the inter-segment area. The septum is distinguished by the fact that it is made of

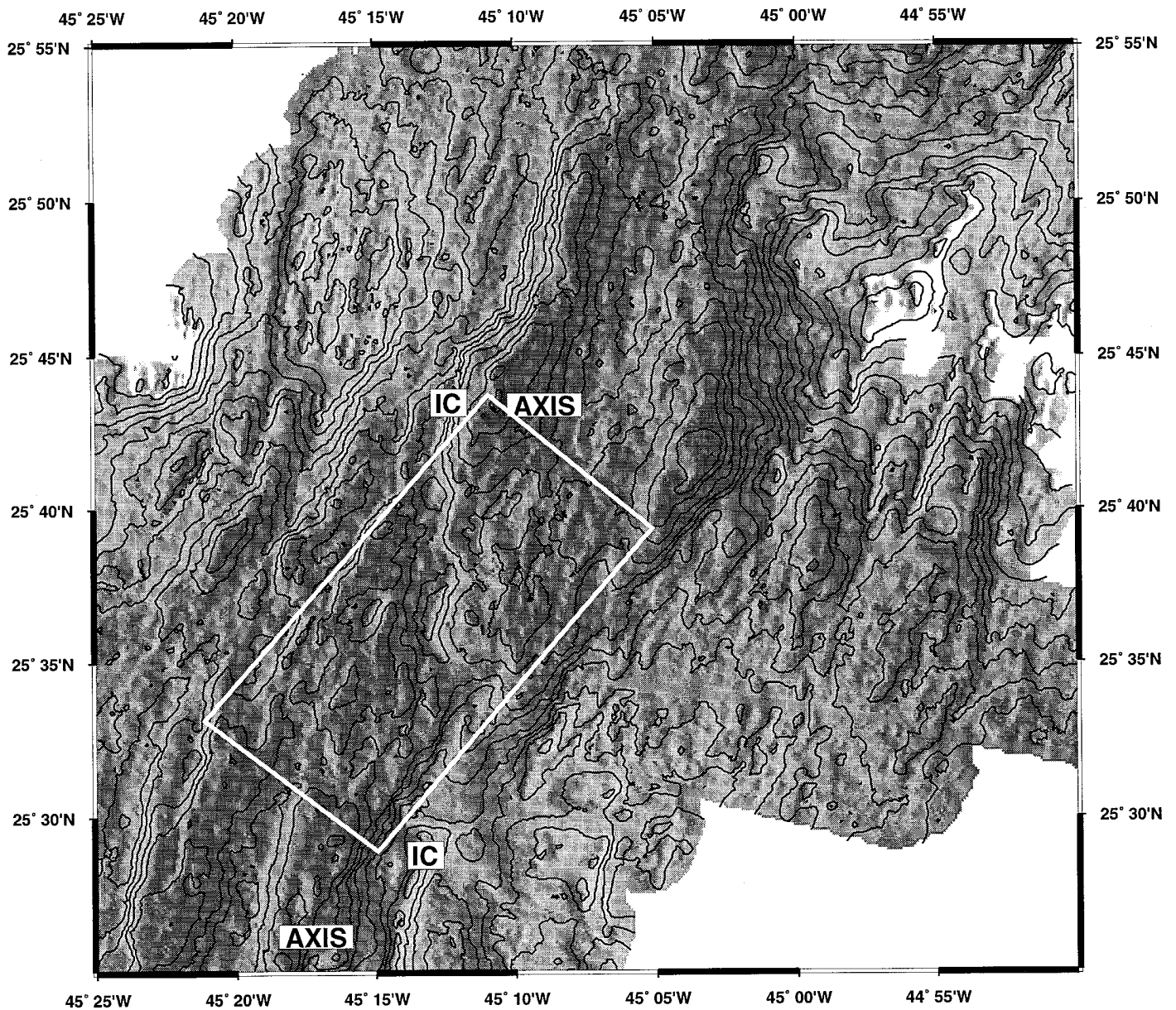


Fig. 4. (a) Gray-scale bathymetric image of the NTD at 25°36' N (Purdy et al., 1990). The contour interval is 50 m. The location of the sidescan coverage is indicated by a white outline on the bathymetry map. Note that the two spreading segments are separated by a high. This is referred to here as a septum, hence septal offset. (b) Photograph of a side-scan sonar (TOBI) mosaic of the NTD at 25°36' N. The mosaic comprises three overlapping swaths. In the area of overlap the swath selected is the one which best illuminates the topography. The track of the TOBI vehicle bisects each swath and is marked by small white parallel time (half hour) lines. The scalloping along the track is an artefact caused by problems with bottom tracking. Data within 500 m of the centre is thus considered to be unreliable. Areas of bright back-scatter represent strata which dips towards the ships track, where linear these are interpreted as faults and where broad as landslides. (c) Geological interpretation of the NTD at 25°36' N. The septal high associated with the NTD is partly volcanic and partly tectonised.

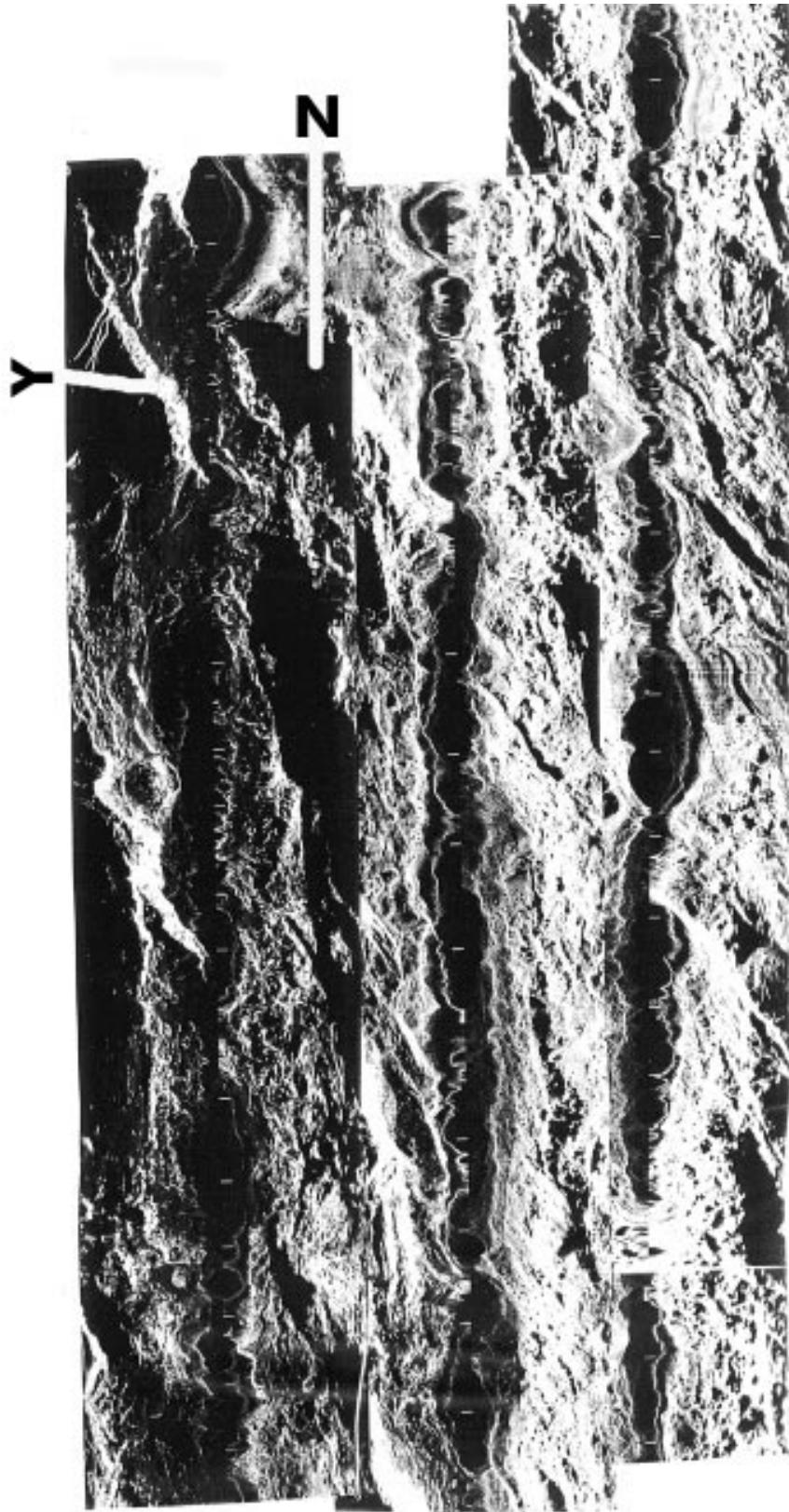


Fig. 4b

X

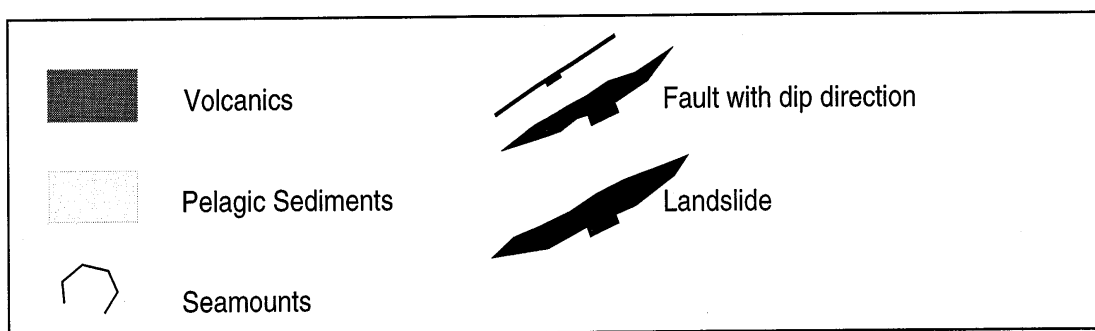


Fig. 4c

closely spaced en echelon fault blocks and has the highest local relief. The zones of lower relief between fault blocks both along the septum and within the segments are characterised by hummocky volcanic features.

A similar septum was identified at 28°51' N. Separating two segments (16 and 17, Figure 2) which show neither an overlap nor an along-axis gap, it comprises

a series of linked bathymetric highs which trend 013°. As in the previous case the side-scan sonar image indicates that these highs are en echelon fault blocks. Again these form part of a continuum of fault blocks oriented 012°–030° which cross-cut the ends of both of the axial volcanic ridges within the segments and intersect the discontinuity. In this case, however, the dominant throw of the faults is to the west.

The septa thus appear to be made of an uplifted section of an array of fault blocks, in which the faults throw uniformly either to the west or east. The orientation of these fault blocks appears to correspond to that of the median valley wall that has undergone the most tectonism. Thus the 25°36' N septum which is characterised by a fault array that throws down to the east is related to a strong fabric in the western flank of the northern segment whereas the 28°51' N septum which has a fault array that throws down to the west is related to a strong fabric in the eastern flank of the southern segment.

Septal Offsets Identified from the Multibeam Bathymetric Data

Other septa have also been recognised from the bathymetric data (Sempéré et al., 1993) and include the NTDs at 25°56' N between segments 8 and 9, 26°17' N between segments 9 and 10, 27°09' N between segments 12 and 13, 27°43' N between segments 13 and 14, 28°15' N between segments 14 and 15, 28°42' N between segments 15 and 16 and 29°23' N between segments 17 and 18 (Table I). Although we do not have side-scan sonar coverage of these septa it has been possible using the bathymetric and gravity data to recognise significant variations in septum style. This allowed their subdivision into two distinct categories, Types 1A and 1B respectively (see Table I). The first of these categories, Type 1A, includes septa marked by a narrow linear high oriented sub-orthogonal to the spreading direction (354°–017°), in which one or both sides is marked by closely spaced contours (Figure 4a). This category includes both of the septa described above for which we have TOBI coverage (25°36' N and 28°51' N) and those at 25°56' N, 26°17' N and 29°23' N (Table I). Of these five septa, all show substantial segment offsets of between 7.2 to 13.4 km, a distinct offset of the median valley, a segment overlap of between 0 and 14.7 km and a discontinuity width of between 0.13 and –16.1 km (Table I). Type 1B septa (Figure 5) are those which comprise a series of isolated highs each of which is marked by closely spaced contours on one or both sides and which together form a broad zone of elevated topography oriented at a high angle to both the spreading and the spreading orthogonal directions (319°–332°). Type 1B septa include those at 27°09' N, 27°43' N, 28°15' N and 28°42' N (Table I). All of these are characterised by substantial segment offsets (9.7–13.7 km), a distinct offset of the median valley, segment overlaps of between 0 and –8.3 km, and a discontinuity width of between 0.92 and 4.75 km (Table I). The septa account for nine of the seventeen NTDs in the study area.

Off-Axis Traces of the Septal Offsets

On the single beam bathymetric maps (Rona, 1976; Rona et al., 1976; Rona and Gray, 1980) and multi-beam bathymetric maps (Sempéré et al., 1993) the Type 1A septal offsets at 25°36' N, 25°56' N, 28°51' N and 29°23' N are associated with off-axis traces marked by the linear alignment of basins and elongate ridges. The basins are characteristic of the off-axial traces of discontinuities (e.g. Sempéré et al., 1993) whilst the ridges are interpreted as possible remnants of previous septa. At the 25°36' N NTD the Brunhes-Matuyama boundary is offset (Sempéré et al., 1993), and the gravity data (Figure 2) shows a well-developed off-axial trace. This suggests that this NTD has persisted through time (Sempéré et al., 1993) although not necessarily as a septal offset nor at its present latitude (Table I). The NTD at 25°56' N shows a similar distinct off-axial trace (Table I, Figure 2). The NTDs at 28°51' N and 29°23' N are also marked by an off-axial trace in the gravity data but this is not as prominent nor as long-lived as those at 25°36' N and 25°56' N. Sempéré et al. (1993) suggested that the 28°51' N and 29°23' N NTDs, though long-lived, were previously associated with a much smaller offset (Table I). Of the Type 1B septal offsets, only the one at 28°42' N has an off-axial trace in the bathymetric data and a weak off-axial trace in the gravity data (Figure 2) which supports long-term stability (Table I).

TYPE 2: EXTENSIONAL SHEAR ZONES

Shear Zone at 24°51' N

This type of discontinuity is represented by the NTDs first identified by Sempéré et al. (1993) at 24°51' N. Using the bathymetric maps of Purdy et al. (1990, Figure 6a), Sempéré et al. (1993) described the NTD as a degenerate transform comprising a right stepping offset of 30 km characterised by two basins and an intra-offset ridge. They considered this to be a second-order discontinuity, accommodated by two short-lived, en echelon, narrow shear zones which paralleled the spreading direction. The intra-offset ridge was thought to be the result of volcanism associated with the extensional jog of the faults (Sempéré et al., 1993). Co-registration of the bathymetric images with side-scan sonar data of the median valley and subsequent detailed analysis of the volcano-tectonic morphology of the inner valley floor has led us to a new interpretation of segment boundaries in the area from 24°39' N to 24°53' N. In particular we re-interpreted the intra-offset ridge as a separate volcano-tectonic segment, which is offset dextrally at its southern termination (24°51' N) by an offset of 14.3 km and at its northern

TABLE I

Summary of non-transform discontinuities characteristics. Additional data from (1) Sempéré et al. (1993), (2) Rona (1976) and (3) Rona and Gray (1980)

| Segments | Latitude | Segment Offset (km) | Segment Overlap (km) | Median Valley Offset (km) | Offset Zone Width (km) | Local Fault Orientation | | | Order | Interpretation | Longevity |
|----------|----------|---------------------|----------------------|---------------------------|------------------------|-------------------------|-----|-----|-----------------|--|---|
| | | | | | | S | N | | | | |
| 1 2 | 24°22' N | 1.5 | 0 | | | 14° | 32° | 3rd | Non-tectonised | Median valley walls are continuous, suggesting that this discontinuity is either recent or has never been associated with a large offset or depth anomaly (1,2,3). | Although this is only a minor offset the along-axis bathymetry and the significant change in morphology does support the existence of two separate spreading segments. |
| 2 3 | 24°39' N | 11 11 | -1.1 1.3 | | | 32° | 32° | 2nd | Shear Zone ? | A broad zone of 'V'-shaped off-axis traces indicate that either one or both of these discontinuities has persisted with time (1,2,3). | The segments are separated by a deep basin which shallows in the mid-section. |
| 3 4 | 24°46' N | 3.7 | 2.9 | | | 32° | 32° | 3rd | Non-tectonised | | Both of these segments are very short and narrow. They are separated by a 200 m deep depression (1). |
| 4 5 | 24°51' N | 14.3 14.3 | -0.5 0 | | | 32° | 32° | 2nd | Shear zone | Evidence suggests that this zone of discontinuities has existed for the last 7 Ma, and that during that time it has migrated along the axis (1,2,3). | The segments are separated by a deep basin which shallows in the mid-section. |
| 5 6 | 24°53' N | 18 18 | -0.3 0 | | | 32° | 15° | ? | Shear zone | | TOBI data indicates that this discontinuity comprises a zone of oblique faulting. |
| 6 7 | 25°20' N | 3 | 0 | | | 15° | 23° | ? | Non-tectonised | Minor deflection of the rift valley walls and off-axis structure indicate that this discontinuity may have existed for some time. | The offset here is disrupted by faults which appear to be propagating north from the median valley walls of the southern segment and south from the median valley walls of the northern segment. |
| 7 8 | 25°36' N | 11 | 7.7 | 5.94 | -9 | 23° | 23° | 2nd | Septum Type A | The B-M boundary is offset and there is a distinct off-axis trace suggesting that this discontinuity has persisted through time (1,2,3). | TOBI data indicates that the septum which is oriented 354° is a tectonic feature comprising a series of fault blocks which dip to the east. The septum is associated with a magnetic high. |
| 8 9 | 25°56' N | 11.5 | 14.7 | 9.24 | -16.1 | 23° | 29° | 2nd | Septum Type A | Very distinct off-axis trace indicates the longevity of this discontinuity (1,2,3). | This is a very narrow septum oriented 010° which comprises isolated highs, interpreted as eastward dipping fault blocks. |
| 9 10 | 26°17' N | 9 | 3.2 | 6.27 | -13.5 | 29° | 27° | 3rd | Septum Type A | Although there is a jog in the present median valley wall there is no evidence to support the existence of this discontinuity through time (1,2) | This offset is associated with a 4 km wide, 4400 m deep basin (1). |
| 10 11 | 26°34' N | 3.4 | 6.5 | | | 27° | 10° | 3rd | Non-tectonised | The present discontinuity is recent although evidence supports the existence of an offset at this locality at some time in the past (1,2,3). | TOBI data shows no evidence of tectonism in association with this discontinuity. |
| 11 12 | 26°56' N | 3.1 | 0 | | | 10° | 20° | 3rd | Non-tectonised | The present discontinuity is marked by a jog in the eastern wall. Off-axis data indicates that this offset is either recent or it has always been small (1). | The magnetics at this latitude display a split high, with one of the magnetic highs located off-axis. |
| 12 13 | 27°09' N | 10.7 | -3.4 | 8.06 | 4.75 | 20° | 20° | 2nd | Septum Type B | There is an along-axis trace which corresponds to this offset but there is no disruption of the B-M boundary (1). | Diffuse septum comprising a series of en echelon linear highs offset in a sinistral manner which combine to form a broad zone oriented 319°. The highs are interpreted as fault blocks which dip to the east. |
| 13 14 | 27°43' N | 11 11 | 0 13 | 5.22 | 1.85 | 20° | 18° | 3rd | Septum Type B | There is only limited evidence to support the existence of this discontinuity through time (1). | Diffuse septum comprising a series of en echelon linear highs offset in a sinistral manner which combine to form a broad zone oriented 332°. The highs are interpreted as fault blocks which dip to the west. |
| 14 15 | 28°15' N | 9.7 | 0 | 3.17 | 0.92 | 18° | 26° | 2nd | Septum Type B | There is an along-axis trace which corresponds to the present offset but there is no disruption of the B-M boundary indicating either that the discontinuity did not exist or it was very small (1). | This discontinuity comprises a 3900 m deep basin (1). |
| 15 16 | 28°42' N | 13.7 | -8.3 | 10.5 | 3.2 | 26° | 30° | 2nd | Septum Type B | Off-axis data indicate that this discontinuity has been persistent through time (1). | This discontinuity comprises a broad high in which there are no dramatic changes in relief. |
| 16 17 | 28°51' N | 7.2 | 0 | 11.62 | 0.13 | 30° | 19° | 2nd | Septum Type A | The off-axis traces indicate that this discontinuity was previously associated with a much smaller offset (1). | TOBI and bathymetric data show this to be a well-developed septum oriented 017°, comprising tilted fault blocks which dip to the west. |
| 17 18 | 29°23' N | 13.4 | 7.13 | 15.97 | -4.6 | 19° | 20° | 2nd | Septum Type A + | Evidence suggests that this discontinuity did exist previously but was associated with a much smaller offset (1). | Very well-developed septum oriented 010° in which the faults appear to dip to the east. |

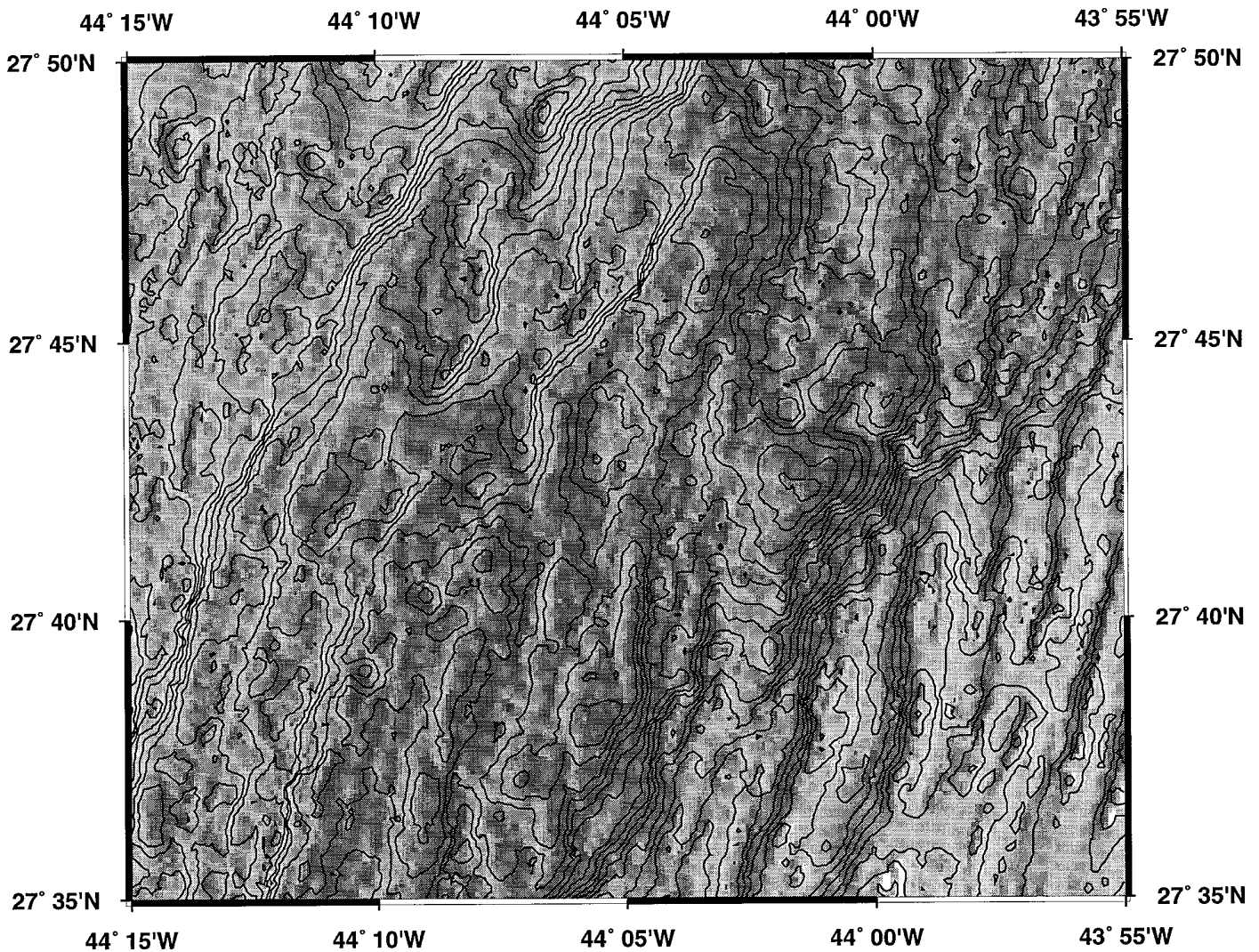


Fig. 5. Gray-scale bathymetric image of the Type B septum at 27°43' N. The contour interval is 50 m. The two spreading segments are separated by a diffuse septum.

termination (24°53' N) by an offset of 18 km (Figure 6a). These represent two separate discontinuities. The segments at 24°51' N overlap by between 0 and -0.5 km and those at 24°53' N by between 0 and -0.3 km (Table I). In both cases the median valley is offset.

Side-scan sonar (TOBI) data are available for the northern section of this area, the offset at 24°53' N, and is shown in Figure 6b. The two offset segments (segments 5 and 6, see Figure 2) are characterised by axial volcanic highs composed of sheet flows, hummocky terrain and isolated seamounts (Figure 6c). Fault scarps adjacent to the segment to the north parallel the axial volcanic highs along most of their length (015°-195°), but undergo a significant change in ori-

entation (032°-222°) proximal to the NTD (Escartin and Lin, 1995). The offset zone itself is characterised by a series of tilted fault blocks oriented 050°-230°. Though hummocky volcanics are seen between the fault blocks these are sedimented and there is little evidence of any recent volcanism. Spreading within this NTD zone is thus dominated by extensional faulting. The distribution of faults and fault blocks is similar to that seen in brittle/ductile shear zones (e.g. Ramsay, 1980) where the imposition of a shear couple across an area causes a local rotation in the stress field and a resultant obliquity of compressional and extensional features. In this case a shear couple has been imposed across the NTD as a result of the

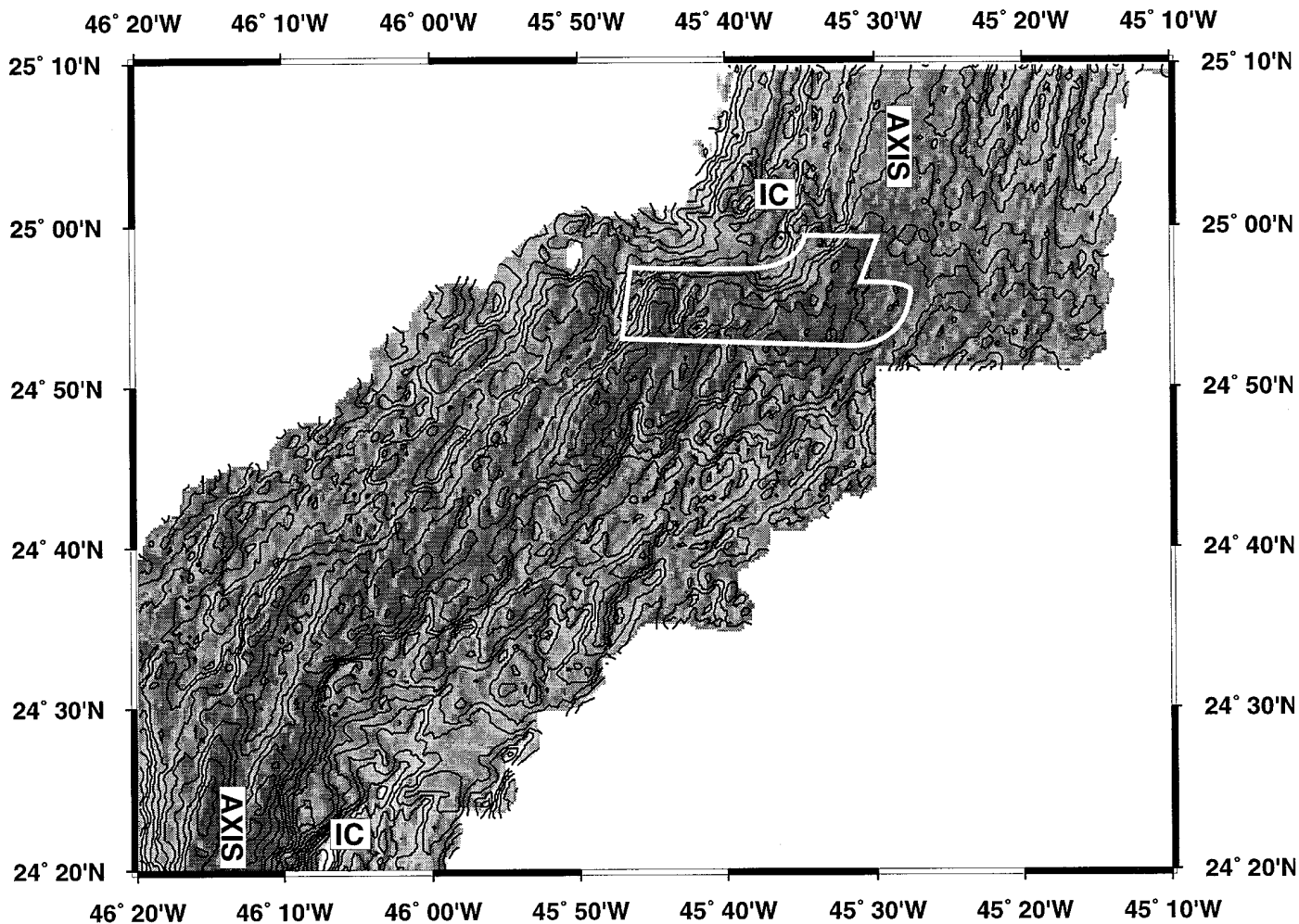


Fig. 6. (a) Gray-scale bathymetric image of the NTDs at 24°20' N and 24°53' N (Purdy et al., 1990). The contour interval is 50 m. The location of the sidescan coverage is indicated by a white outline on the bathymetry map. (b) Photograph of a side-scan sonar (TOBI) mosaic of the NTD at 24°53' N (see figure caption 4b for details). The offset is characterised by oblique extensional fractures and faults. These show up as areas of bright back-scatter where they dip towards the ships track, and shadow where they dip away from it. (c) Geological map of the NTD at 24°53' N. The NTD is characterised by extensional faults/fractures similar to those seen in brittle/ductile shear zones. The faults trend 050°–230° at 50° to the spreading direction. Their orientation is consistent with them having been formed in an extensional shear zone.

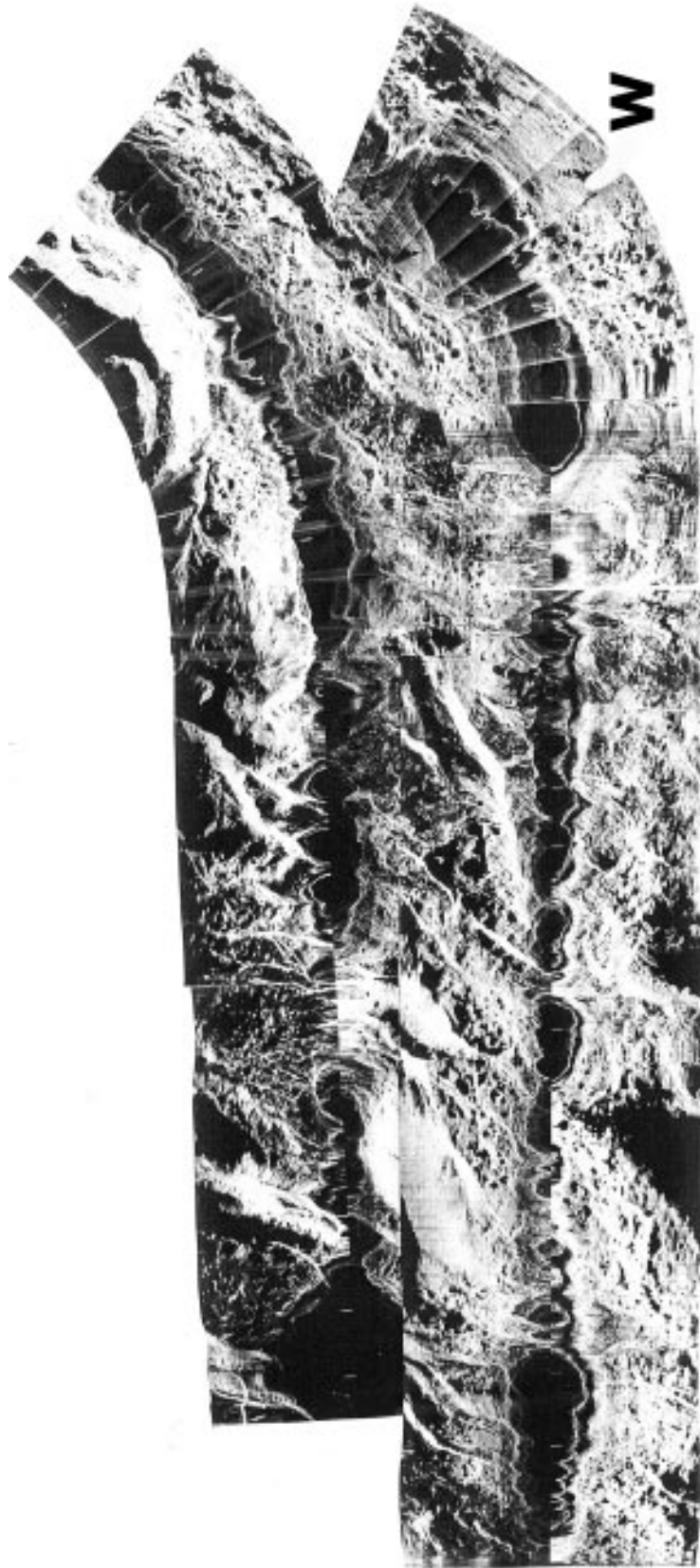


Fig. 6b



Fig. 6c

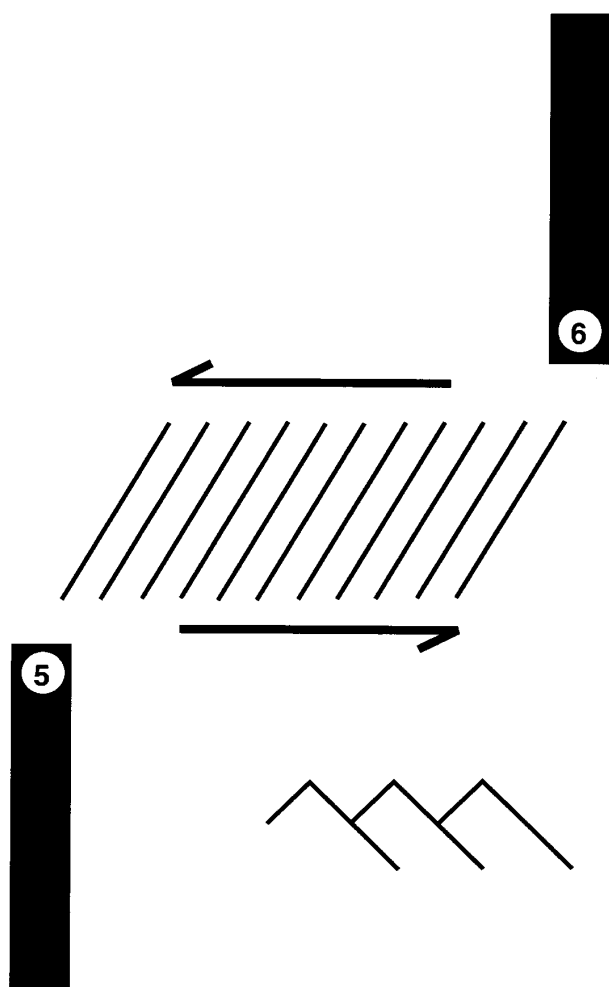


Fig. 7. Line drawing showing an interpretation of the NTD at 25°36' N as a shear zone. The opposing spreading directions of the two segments 5 and 6 (marked by the solid black lines) impose a shear across the discontinuity resulting in extensional faulting at a high angle to the spreading normal direction.

opposed spreading directions of the two segments (5 and 6, Figure 7). The resultant fault pattern is thus oblique to the spreading normal direction.

The obliquity of the fault pattern has also been recognised from the bathymetric data (Rona and Gray, 1980; Escartin and Lin, 1995) and is seen to cover a much larger area, extending from 24°53' N to 24°39' N. This area contains three separate segments (13–21 km in length) and four discontinuities at 24°39' N, 24°46' N, 24°51' N and 24°53' N with segment offsets of 3.7–18 km and overlaps of –1.1 to 2.9 km (Table I). It is characterised by having a much lower relief (see Figure 5 in Rona and Gray, 1980, and Figure 3b in Sempéré et al., 1993) than that seen in adjacent areas of the ridge

axis. In particular it lacks much of the higher relief normally associated with the crestal mountains and inner corner highs. It was thus not possible to measure the width of the zones of discontinuity.

Off-Axis Traces

Off-axis traces in the bathymetric data (Purdy et al., 1990; Rona, 1976) and gravity data (Sandwell and Smith, 1992) indicate that the present distribution of segments and offsets is relatively new. Basins which align to form troughs oriented 095°–115° (Sempéré et al., 1993) and 265°–275° (Rona, 1976) to the east and west of the ridge axis respectively at 24°51' N indicate that an NTD has been present near this latitude, though not necessarily in its present form for at least the past 7 Ma (Sempéré et al., 1993). It is also only possible to distinguish one off-axis trace, which because of its width cannot be directly attributed to either the NTD at 24°51' N or that at 24°53' N. Either one or both may have existed through time. The NTD at 24°46' N has no offset trace (Sempéré et al., 1993) indicating that this is either a relatively recent discontinuity or that the offset has always been too small and/or migratory to cause long-term disruption at a given latitude. Finally the NTD at 24°39' N is marked by a 'v' shaped off-axis trace indicating that this discontinuity has persisted with time (Rona, 1976; Rona and Gray, 1980; Sempéré et al., 1993).

Off-axis magnetic anomaly and bathymetric data for this area (Tucholke and Schouten, 1989) clearly shows that prior to 22 Ma (between magnetic anomalies 13 and 6) segments two and six were originally adjacent and offset by a single discontinuity. However, by 14 Ma (between magnetic anomalies 6 and 5) the two segments had begun to retreat from one another along the axis, leaving a magmatic gap. This process of retreat appears to have continued to the present day. Segments two and six are now separated by approximately 26 km (measured N/S) of relatively low lying relief and three short spreading segments oriented at an angle to the overall ridge trend (Figure 6).

It is thus proposed that the NTD at 24°53' N is only the northern termination of a much wider zone of shear which extends from 24°39' N to 24°53' N and marks the discontinuity between segments two and six. This shear zone is dominated by tectonism with magmatism being restricted to a series of short, oblique, en echelon segments (Segments 3, 4 and 5, Table I, Figure 2).

TYPE 3: NON-TECTONISED DISCONTINUITY

The NTD at 26°34' N between segments 10 and 11 (Figure 8a–c) represents the third distinct type of offset

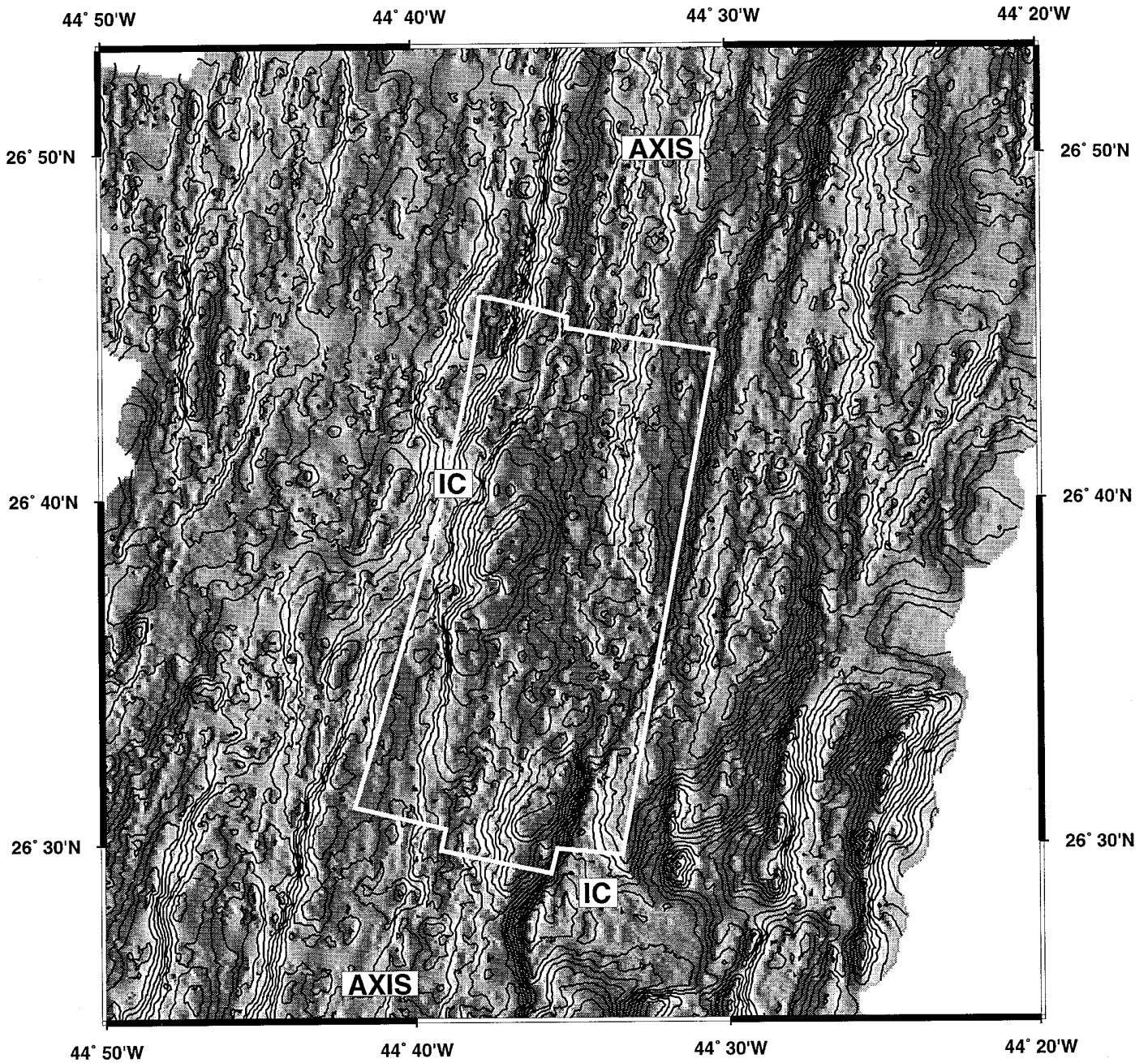


Fig. 8. (a) Gray-scale bathymetric image of the NTD at 26°34' N (Purdy et al., 1990). The contour interval is 50 m. The location of the sidescan coverage is indicated by a white outline on the bathymetry map. (b) Photograph of a side-scan sonar (TOBI) mosaic of the NTD at 26°34' N (see figure caption 4b for details). (c) Geological map of the NTD at 26°34' N. The NTD here is covered by surface volcanism which masks any structure that may exist at depth. This is therefore referred to as a non-tectonised NTD.

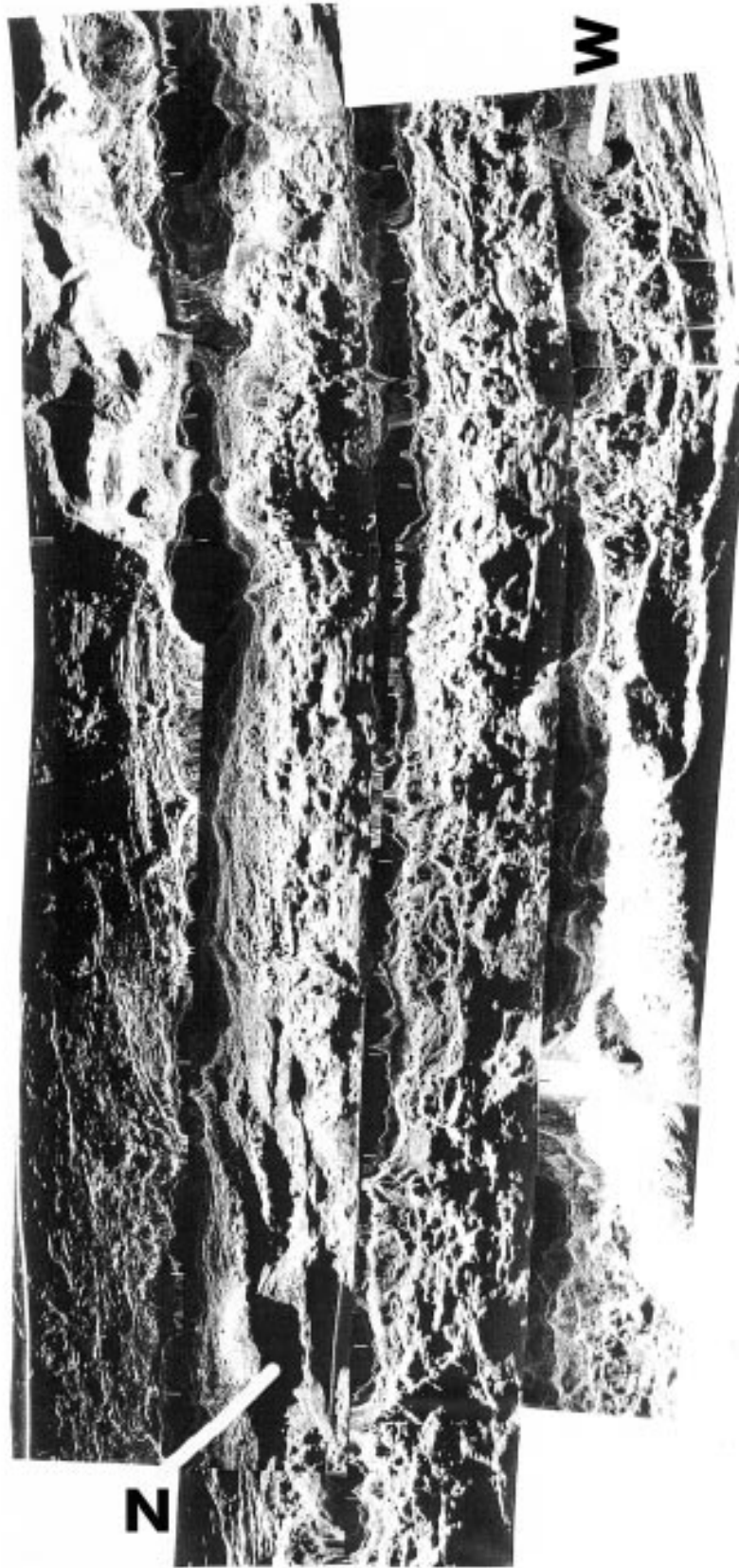


Fig. 8b

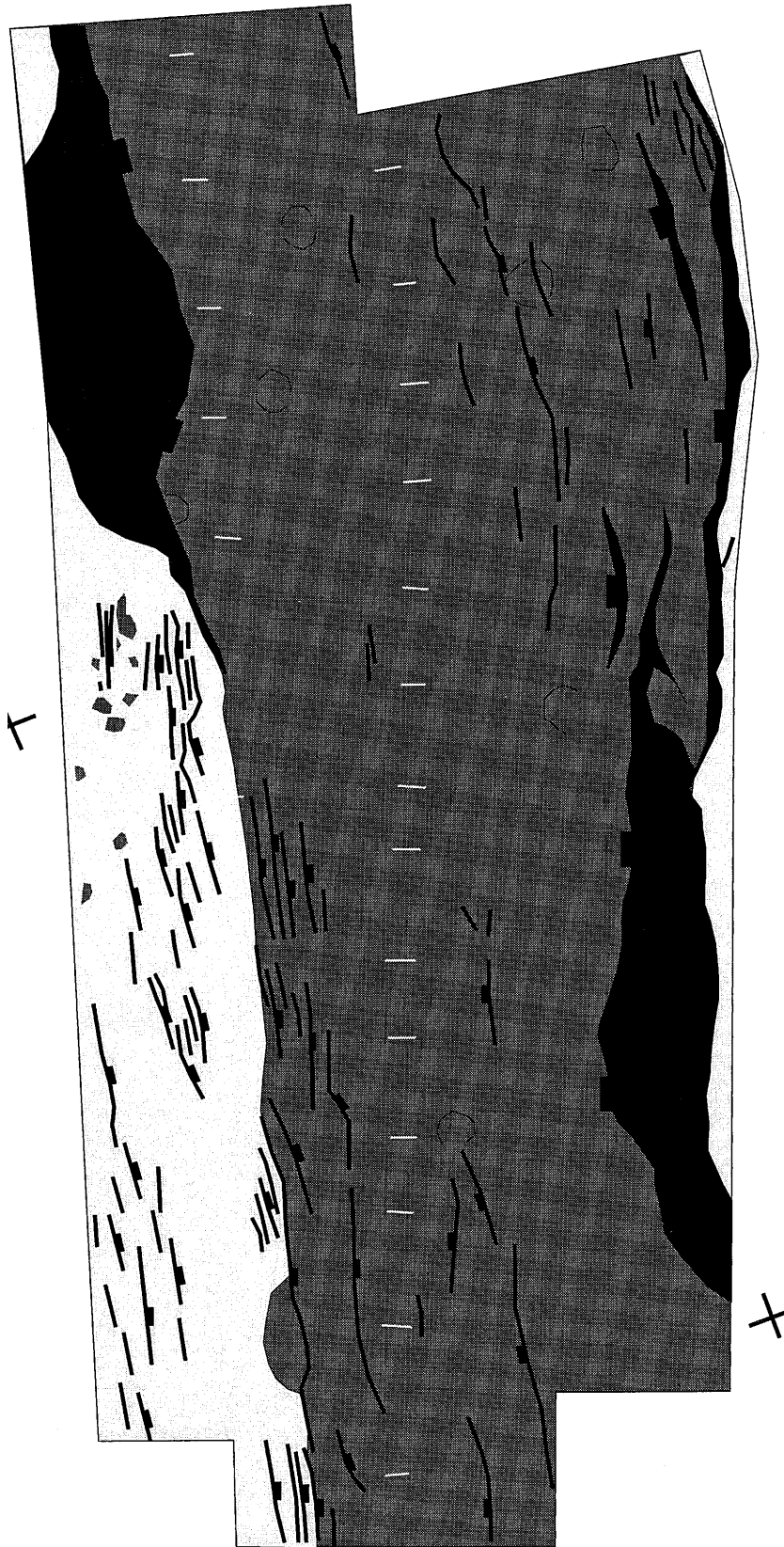


Fig. 8c

identified. Sempéré et al. (1993) described this NTD as a third order discontinuity. It is characterised by a right stepping segment offset of 3.4 km and an along axis overlap of 6.5 km (Figure 8a). Side-scan sonar coverage of this discontinuity provides very little insight into the nature of the offset (Figure 8b–c). Both of the adjacent segments have robust axial volcanic ridges which are dominated by hummocky volcanic ridges and small seamounts. This, combined with the small offset between the segments and their along-axis overlap, masks any structure that may exist to accommodate the opposed spreading directions across the discontinuity. This type of discontinuity is thus referred to as a non-tectonised NTD. At present the median valley walls are continuous through the discontinuity indicating that this offset is recent or has always been small (Sempéré et al., 1993) although chains of bathymetric lows aligned at 111° to the east and 264° to the west of the axis indicate that another discontinuity may have existed at this latitude in the past. Other non-tectonised NTDs include those at $24^\circ 22'$ N between segments 1 and 2, $25^\circ 20'$ N between segments 6 and 7, and $26^\circ 56'$ N between segments 11 and 12. These have segment offsets of between 1.5 and 3.1 km and neither an along-axis overlap or an along-axis gap (Table I). These NTDs are characterised by only small offsets of the median valley walls and they have no off-axis trace in the gravity data (Figure 2) indicating that the offset has always been small, or that the discontinuity is recent or that it has been very mobile. Non-tectonised NTDs account for four of the seventeen NTDs in the study area.

Controls on NTD Style

Three distinct types of NTD have been identified between the Kane and Atlantis fracture zones. The data in Table I show that these types vary not only in their morphology but also in the amount of segment offset and segment overlap, the width of the zone of discontinuity and their longevity; but what ultimately controls their tectonic style? The answer probably lies in the mechanical properties of the lithosphere at the discontinuity. Sclater and Francheteau (1970) and Parsons and Sclater (1977) demonstrated that the thickness of oceanic lithosphere is age related. As the lithosphere moves away from the ridge axis it cools, leading to lithospheric contraction, increasing oceanic depth and an increase in density. Since the lithosphere–asthenosphere boundary is temperature-related, the cooling also results in an increase in lithospheric thickness. This has implications for the mechanical strength

of the lithosphere. Young lithosphere at the ridge axis is weaker since it is thinner and hotter than the lithosphere off-axis. The mechanical strength of the lithosphere thus increases with distance from the ridge axis. The properties of the lithosphere will also vary across ridge discontinuities as lithosphere of different ages is juxtaposed (e.g. Blackman and Forsyth, 1991; Morris and Detrick, 1991). Large offsets will thus show substantial variations in lithospheric thickness and inferred strength (e.g. Sclater et al., 1971; Macdonald and Fox, 1983) across the discontinuity whilst at small offsets this variation will be small or negligible.

The non-tectonised NTDs are characterised by small segment offsets (<4 km, age offset <0.26 Ma), zero or positive overlaps, no off-axis trace and negligible median valley wall offsets. In this case the lithosphere at the discontinuity is young and there are no major changes in lithospheric thickness nor in the mechanical properties of the lithosphere across the NTD (Figure 9a). The lack of an off-axis trace for any of these offsets implies that they are either ephemeral or consistently small offset discontinuities and that any variation in spreading direction is accommodated by local segment adjustment within the confines of the median valley.

The septal offsets are more numerous and more diverse than the non-tectonised NTDs. Septa are associated with larger segment offsets (7 and 14 km) and thus larger age offsets (0.5 and 1 Ma). In this case lithospheric thickness and strength can vary significantly both along and across the NTD. The two types of septal offsets identified show similar segment offsets. The main difference between them is the amount of segment overlap and the width of the zone of discontinuity. Type 1B septal offsets are associated with zero or negative overlaps. In this case the zone of discontinuity is narrow and the lithosphere associated with each segment is offset along a semi-discrete boundary (Figure 9b). The Type 1A septa, on the other hand, are associated with zero or positive overlaps. Such overlaps result in an extensive area of relatively young lithosphere at the discontinuity separating the older lithosphere at the inside corner highs by a considerable distance (Figure 9c). This results in a much wider zone of discontinuity. Since the septa are zones of elevated fault terrain which appear to link the inner corner highs, it follows from the contrasting properties of the two types of NTD that whilst Type 1B septa are oriented at a high angle to the trend of the median valley faulting and the overall ridge trend, Type 1A septa are oriented at a low angle to the fault trend and the overall ridge trend (Figures 9b and c).

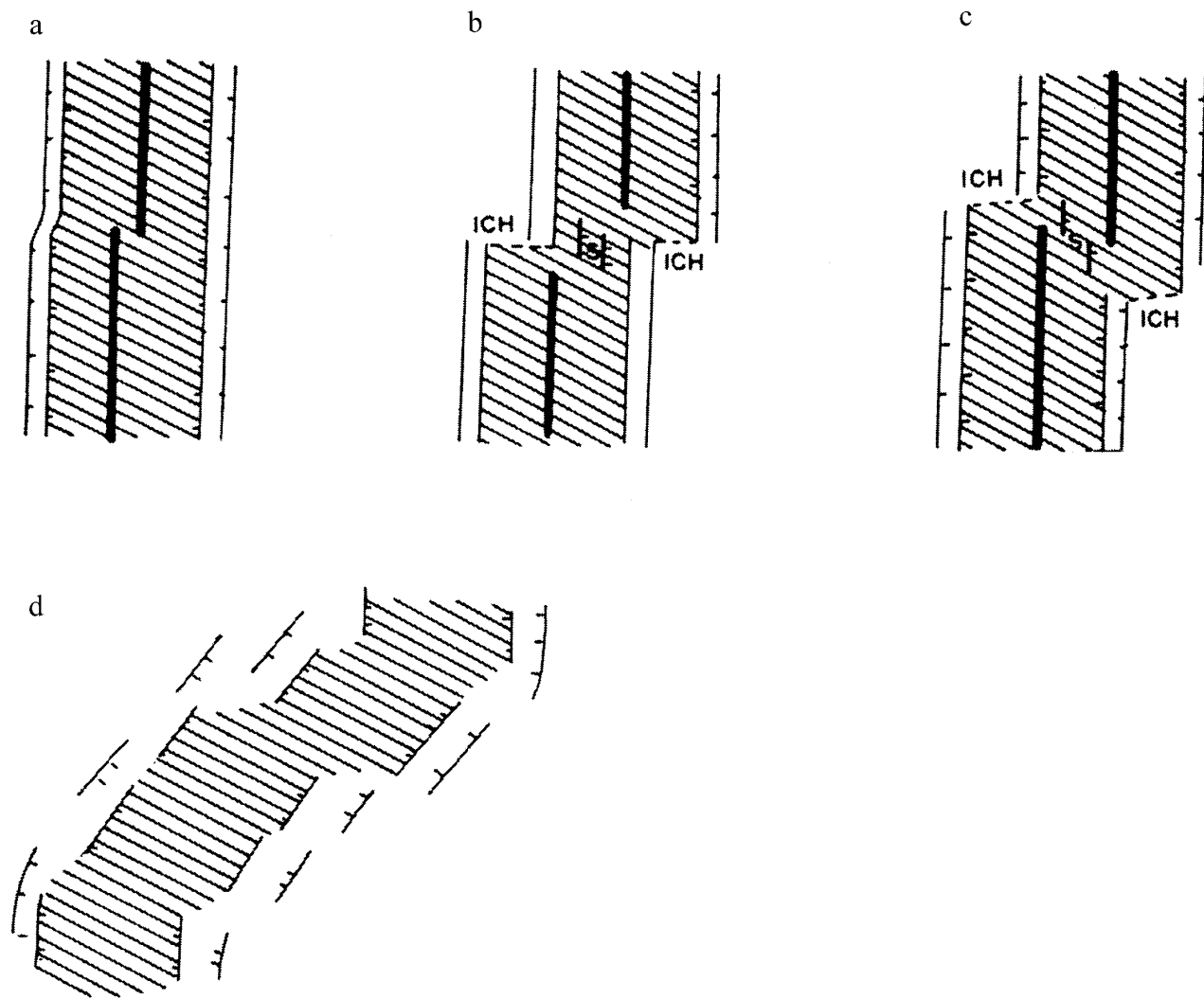


Fig. 9. Line drawings showing the different types of NTDs as part of a continuum of discontinuities accommodating the offset spreading segments (marked by the solid black lines). ICH = Inner corner high, S = Septum, the hatched area represents the median valley floor and the lines with ticks represent extensional faults (the ticks are on the downthrown side). (a) Non-tectonised NTD, (b) Type B septum, (c) Type A septum, (d) Brittle-ductile shear zone.

The elevation of the septa relative to the adjacent area also appears to be linked to their relationship with the inside corner highs. The differences in the mechanical strength between the older and younger lithosphere at the inside corner highs at Type 1A septa allows the inner corner highs to rise to greater elevations than at Type 1B septa where the age difference and hence mechanical strength of the lithosphere across the inner corner is not as significant. Type 1A septa show greater relief than Type 1B septa indicating that the septal uplift may be a by-product of the dy-

namic force responsible for the uplift of the inner corner highs.

The brittle-ductile shear zone 24°39' N to 24°53' N represents the least common though most extensive of the NTDs identified (Figure 9d). This is a long-lived structure which developed in response to opposing shear directions across a discontinuity in which the offsets were large and overlaps between the short en echelon segments, small or negative (Table I). The key to the development of this group of NTDs, however, lies not in the amount of offset or overlap between

segments at present but in the past motion of the plates and hence distribution of segments. On a regional scale the relative plate motion across the ridge has undergone a 10° anticlockwise rotation from 110° to 100° during the last 22 Ma (Tucholke and Schouten, 1989). The result of this was to put the existing transform faults into extension (Tucholke and Schouten, 1989) and to change the orientation and distribution of segments and hence NTDs. This led to a retreat of Segments 2 and 6 resulting in an along-axis gap in magmatism. Initially the lithosphere in this area would have cooled, becoming denser and thicker. The continued motion of the plates, however, resulted in stress across the area producing fracture and tectonic thinning of the brittle lithosphere. As the upper lithosphere was thinned, the warmer lower lithosphere and asthenosphere would rise (e.g. McKenzie, 1978), the resultant drop in pressure would have led to localised melting and the formation of the new segments (3–5) within the shear zone. The orientation of these segments is now controlled by the local tectonic fabric which is oblique to the overall ridge trend.

NTD Evolution

Any view of a spreading ridge provides only a snapshot of the processes active at the ridge at any one time. As the ridge develops through time in response to changes in the spreading direction and/or magma supply, individual segments and groups of segments must evolve in order to accommodate the new regime. As the segments evolve so too must the NTDs, which are fundamentally ephemeral accommodating structures between the offset spreading centres. Thus, NTDs form a continuum of possible offset structures which accommodate changes in ridge morphology. These structures vary from the ephemeral to the persistent but all must be capable of evolving through time.

The Type 3 non-tectonised NTDs probably evolve through the localised propagation and retreat of segments within the confines of the median valley floor, allowing the new crust created at each segment to be carried off axis. However, since there are no off-axis traces of the non-tectonised NTDs nor any visible tectonic structure in the median valley it is hard to investigate their evolution in detail.

Within the Type 1 NTDs, the septa cannot be steady state features of the ridge axis. At some point the elevated fault blocks that make up the septa must be carried off axis. This may be achieved through propagation or retreat of the neovolcanic zones, thus carrying the septa off into the off-axis region intact. At

Type 1A septal offsets, where the spreading segments overlap, one segment must retreat to allow the fault blocks to be accreted to one plate and moved off-axis. This process would account for the narrow isolated ridges which are offset from the inside corner highs and which run from the inner corner wall into the median valley (Figure 4a). Eventually such a relic septum must subside as it is removed from the region of the inside corner high and from the dynamic force responsible for its uplift. Such segment propagation or retreat (whilst maintaining segment offset) may also result in a Type 1B septa evolving into a Type 1A septa or vice versa as the nature of the overlap changes. This may have happened to the septal offset at 28°51' N which, although categorised as a Type 1A septal offset on the basis of its geometry, shares many characteristics with the Type 1B septa. However, this evolution may not be common, since the Type 1A and Type 1B septal offsets have different off-axis signatures, and thus different long-term histories.

For these reasons we suggest that NTDs are spatially and temporally variable features. They do not reflect plate motion in the same way as transform faults but rather respond to the way in which individual segments and groups of segments rearrange themselves in response to mantle diapirism, melt driven processes, changes in spreading direction, gravitational spreading forces and crack propagation (Hey et al., 1980; Macdonald et al., 1984, 1991; Crane, 1985; Morgan and Parmentier, 1985; Lonsdale, 1989). These long- and short-term changes are thought to be reflected in the spatial distribution of the off-axis traces of the segments and offsets (e.g. Johnson and Vogt, 1973; Rona, 1976; Rona and Gray, 1980; Schouten et al., 1985; Kleinrock, et al., 1992a, b; Rommevaux et al., 1994).

Spatial Distribution of the Different Types of NTD

On a larger scale the spatial distribution of the different types of NTD raises some interesting points. Figure 2 shows this distribution. Most of the NTDs of a given type are clustered in groups. The brittle ductile shear zone occupies a zone from 24°39' N to 24°53' N. The Type 1B septal offsets occur in a group between 27°09' N and 28°42' N. The Type 1A septal offsets occur in two groups between 25°36' N and 26°17' N, and 28°51' N and 29°23' N, respectively, and the non-tectonised NTDs which occur at 24°22' N, 25°20' N and between 26°34' N and 26°56' N. This grouping appears to be related to the orientation of the overall ridge trend relative to the spreading normal direction (010°, Tucholke and

Schouten, 1989). The non-tectonised Type 3 NTDs lie along sections of the ridge which are almost parallel (008°–013°) to the bulk ridge trend. Type 1A and Type 1B septal offsets lie along sections of the ridge oriented at a higher angle to the bulk ridge trend (at approximately 033° and 028°, respectively) whilst the Type 2 shear zone lies along a section of the ridge oriented at 055°. Except for the segments within and adjacent to the Type 2 shear zone, individual spreading segments are oriented parallel or sub-parallel to the spreading normal direction. Segments that lie along sections of the ridge that are orthogonal to the spreading direction will have small offsets and minor off-axial traces whilst those that lie along sections of the ridge at a progressively higher angle to the spreading direction will have larger offsets and stronger off-axial traces. Since the offset controls the age distribution of the lithosphere, its strength and ultimately the style of NTD, it follows that the orientation of the ridge is important in determining the style of discontinuity.

Conclusions

NTD form a continuum of accommodating structures whose geometry is primarily controlled by the segment offset and overlap. Measurements of segment offset suggest that there are critical values at which the style of discontinuity changes. The first of these is the offset (4 to 7 km) at which Type 3 non-tectonised NTDs give way to Type 1 or Type 2 offsets. At this stage the opposing spreading directions of the two segments can no longer be accommodated within a continuous single median valley. Another critical offset (20 to 30 km) at which Type 1 septal offsets and Type 2 shear zones give way to transform faults occurs where lithospheric age and hence thickness/mechanical strength precludes the propagation of segments across the discontinuity (e.g. Rona and Gray, 1980). Variations in segment overlap do not control the grouping of types of NTDs. They do, however, control the style of a NTD within a particular group.

Acknowledgements

We would like to take this opportunity to thank all of the scientists who participated in the CD65 cruise. Those not authors here are Martin E. Dougherty, Chris Macleod, Scott. C. Garland, Jane Keeton, Benjamin Brooks and Rachel Pascoe. We would also like to thank the captain and the crew of the RRS *Charles Darwin*, the TOBI personnel (Nick Millard and Chris

Flewellen) and participants from the NERC scientific services (Robert Lloyd, Dave Booth, Mike Sampson and Andy Hill).

We would like to acknowledge the following research bodies for supporting this research: NERC for funding the cruise, The Royal Society, London and AUB, Lebanon (SS), NSF grant number OCE9012576 (JL), ONR(DKS).

References

- Bercovici, D., Dick, H. J. B., and Wagner, T. P., 1992, Non-Linear Viscoelasticity and the Formation of Transverse Ridges, *J. Geophys. Res.* **97**, 14,195–14,206.
- Blackman, D. K. and Forsyth, D. W., 1991, Isostatic Compensation of Tectonic Features of the Mid-Atlantic Ridge: 25°–27°30' S, *J. Geophys. Res.* **96**, 11,741–11,758.
- Brozena, J. and Chayes, D., 1988, A Sea Beam Study of the Mid-Atlantic Ridge, 15°–17° S, *Eos, Trans., Amer. Geophys. Union* **69**, 1494 (Abstract).
- Carbotte, S., Welch, S. M., and Macdonald, K. C., 1991, Spreading Rates, Rift Propagation and Fracture Offset Histories During the Past 5 my on the Mid-Atlantic Ridge 25°–27°30' S and 31°–34°30' S, *Marine Geophys. Res.* **13**, 51–80.
- Collette, B. J., 1986, Fracture Zones in the North Atlantic: Morphology and a Model, *J. Geol. Soc. Lond.* **143**, 763–774.
- Crane, K., 1985, The Spacing of Rift Axis Highs: Dependence Upon Diapiric Processes in the Underlying Asthenosphere? *Earth Planet Sci. Lett.* **72**, 405–414.
- Dick, H. J. B., Schouten, H., Meyer, P. S., Gallo, D. G., Bergh, H., Tyce, R., Patriat, P., Johnson, K. T. M., Snow, J., and Fisher, A., 1991, Tectonic Evolution of the Atlantis II Fracture Zone, *Proc. ODP. Scientific Results* **118**, 359–398.
- Escartin, J. and Lin, J., 1995, Ridge Offsets, Normal Faulting, and Gravity Anomalies of Slow Spreading Ridges, *J. Geophys. Res.* **100**, 6163–6177.
- Flewellen, C., Millard, N., and Rouse, I., 1993, TOBI, a Vehicle for Deep Ocean Survey, *J. Elect. and Comm. Eng.* **April**, 85–93.
- Fox, P. J., Grindlay, N. R., and Macdonald, K. C., 1991, The Mid-Atlantic Ridge (31°–34° S): Temporal and Spatial Variations of Accretionary Processes, *Marine Geophys. Res.* **13**, 1–20.
- Fox, P. J. and Gallo, D. G., 1986, The Geology of the North Atlantic Transform Plate Boundaries and Their Aseismic Extensions, in Vogt, M. and Tucholke, B. (eds.), *Decade of North American Geology*, Geol. Soc. Am., pp. 157–172.
- Gente, P., Ceuleneer, G., Durand, C., Pockalny, R., Deplus, C., and Maia, M., 1992, Propagation Rate of Segments Along the Mid-Atlantic Ridge Between 20°–24° (SEADMA I Cruise), *Eos, Trans., Amer. Geophys. Union.* **73**, 569.
- Gente, P., Pockalny, R. A., Durand, C., Deplus, C., Maia, M., Ceuleneer, G., Mevel, C., Cannat, M., and Laverne, C., 1995, Characteristics and Evolution of the Segmentation of the Mid-Atlantic Ridge Between 20° N and 24° N During the Last 10 Million Years, *Earth Planet Sci. Lett.* **129**, 1–4, 55–71.
- Grindlay, N. R., Fox, P. J., and Macdonald, K. C., 1991, Second-Order Ridge Axis Discontinuities in the South Atlantic: Morphology Structure and Evolution, *Marine Geophys. Res.* **13**, 21–50.
- Hey, R. N., 1977, A New Class of Pseudofaults and Their Bearing on Plate Tectonics: A Propagating Rift Model, *Earth Planet Sci. Lett.* **37**, 321–325.

- Hey, R. N., Duennebieber, F. K., and Morgan, W. J., 1980, Propagating Rifts on Mid-Ocean Ridges, *J. Geophys. Res.* **85**, 2647–2658.
- Hey, R. N., Kleinrock, M. C., Miller, S. P., Atwater, T. M., and Searle, R. C., 1986, Sea Beam/Deep-Tow Investigations of an Active Oceanic Propagating Rift System, Galapagos 95.5° W, *J. Geophys. Res.* **91**, 3369–3393.
- Johnson, G. L. and Vogt, P. R., 1973, Mid-Atlantic Ridge from 47° to 51° N, *Geol. Soc. Am. Bulletin* **84**, 3443–3462.
- Karson, J. A., 1990, Accommodation Zones and Transfer Faults: Integral Components of Mid-Atlantic Ridge Extensional Systems, in Peters, T. J., Nicolas, A., and Coleman, R. G. (eds.), *Ophiolite Genesis and the Origin of the Oceanic Lithosphere*, Kluwer Academic Publishers, Dordrecht, pp. 21–38.
- Kleinrock, M. C. and Hey, R. N., 1989, Tectonics of the Failing Spreading System Associated with the 95.5° W Galapagos Propagator, *J. Geophys. Res.* **94**, 13,839–13,857.
- Kleinrock, M. C., Tucholke, B. E., and Lin, J., 1992a, HAWAII MR1 Sidescan Sonar Survey of the Mid-Atlantic Ridge Rift Valley From 25°27' N to 27°00' N, *Eos, Trans., Amer. Geophys. Union* **73**, 43, 567.
- Kleinrock, M. C., Tucholke, B. E., Lin, J., and Tivey, M. A., 1992b, The Trace of Non-Transform Offsets and the Evolution of Mid-Atlantic Ridge Spreading Segments Between 25°25' N and 27°10' N Over the Past 30 my, *Eos, Trans., Amer. Geophys. Union* **73**, 538.
- Kuo, B. Y., Phipps-Morgan, J., and Forsyth, D. W., 1984, Asymmetry in Topography of the Crestal Mountains Near a Ridge-Transform Intersection, *Eos, Trans., Amer. Geophys. Union* **65**, 274.
- Kuo, B. Y. and Forsyth, D. W., 1988, Gravity Anomalies of the Ridge-Transform System in the South Atlantic Between 31 and 34.5° S: Upwelling Centres and Variations in Crustal Thickness, *Marine Geophys. Res.* **10**, 205–232.
- Lin, J., Purdy, G. M., Schouten, H., Sempéré, J. C., and Zervas, C., 1990, Evidence from Gravity Data for Focused Magmatic Accretion Along the Mid-Atlantic Ridge, *Nature* **344**, 627–632.
- Lonsdale, P., 1986, Comments on the 'East Pacific Rise from Siqueiros to Orozco Fracture Zones: Along Strike Continuity of Axial Neovolcanic Zone and Structure and Evolution of Overlapping Spreading Centres' by Macdonald et al., 1984, *J. Geophys. Res.* **91**, 10493–10499.
- Lonsdale, P., 1989, Segmentation of the Pacific-Nazca Spreading Center, 1° N–20° S, *J. Geophys. Res.* **94**, 12,197–12,225.
- McAllister, E. and Cann, J. R., 1996, Initiation and Evolution of Boundary Wall Faults Along the Mid-Atlantic Ridge, 25–29° N, in Macleod, C. J., Tyler, P. A., and Walker, C. L. (eds.), *Tectonic, Magmatic, Hydrothermal and Biological Segmentation of Mid-Ocean Ridges*, *J. Geol. Soc. Lond. Spec. Pub.* **118**, 29–48.
- Macdonald, K. C., 1986, The Crest of the Mid-Atlantic Ridge: Models for Crustal Generation Processes and Tectonics, in Vogt, P. and Tucholke, B. (eds.), *Decade of North American Geology*, Geol. Soc. Am., pp. 51–68.
- Macdonald K. C. and Luyendyk, B. P., 1977, Deep-Towed Studies of the Structure of the Mid-Atlantic Ridge Crest Near 37° N, *Geol. Soc. Am. Bull.* **88**, 621–636.
- Macdonald, K. C. and Fox, P. J., 1983, Overlapping Spreading Centres: New Accretion Geometry on the East Pacific Rise, *Nature* **302**, 55–58.
- Macdonald, K. C., Sempéré, J. C., and Fox, P. J., 1984, The East Pacific Rise From the Siqueiros to the Orozco Fracture Zone: Along Strike Continuity of the Neovolcanic Zone and the Structure and Evolution of Overlapping Spreading Centers, *J. Geophys. Res.* **89**, 6049–6069.
- Macdonald, K. C., Sempéré, J. C., and Fox, P. J., 1986, Reply: The Debate Concerning Overlapping Spreading Centers and Mid-Ocean Ridge Processes, *J. Geophys. Res.* **91**, 10501–10511.
- Macdonald, K. C., Fox, P. J., Perram, L. J., Eisen, M. F., Haymon, R. M., Miller, S. P., Carbotte, S. M., Cormier, M. H., and Shor, A. N., 1988, A New View of the Mid-Ocean Ridge From the Behaviour of Ridge Axis Discontinuities, *Nature* **335**, 217–225.
- Macdonald, K. C., Scheirer, D. S., and Carbotte, S. M., 1991, Mid-Ocean Ridges: Discontinuities, Segments and Giant Cracks, *Science* **253**, 986–994.
- McKenzie, D. P., 1978, Some Remarks on the Development of Sedimentary Basins, *Earth Planet Sci. Lett.* **40**, 25–32.
- McKenzie, D. P., 1986, The Geometry of Propagating Rifts, *Earth Planet Sci. Lett.* **77**, 176–186.
- Morgan, J. P. and Parmentier, E. M., 1985, Causes and Rate-Limiting Mechanisms of Ridge Propagation: A Finite Mechanics Model, *J. Geophys. Res.* **90**, 8603.
- Morris, E. and Detrick, R. S., 1991, Three-Dimensional Analysis of Gravity Anomalies in the MARK Area, Mid-Atlantic Ridge 23° N, *J. Geophys. Res.* **96**, 4355–4366.
- Parsons, B. and Sclater, J. G., 1977, An Analysis of the Variation of Ocean Floor Bathymetry and Heat Flow with Age, *J. Geophys. Res.* **82**, 803–827.
- Phillips, J. D. and Flemming, H. S., 1977, Multibeam Sonar Study of the Mid-Atlantic Ridge Rift Valley 36°–37° N, *Geol. Soc. Am. Bull.* **88**, 1–5.
- Phipps-Morgan, J. and Forsyth, D. W., 1988, Effects of Layering and Anisotropy on Fault Geometry, *J. Geophys. Res.* **93**, 2955–2966.
- Purdy, G. M., Sempéré, J. C., Schouten, H., Dubois, D., and Goldsmith, R., 1990, Bathymetry of the Mid-Atlantic Ridge, 24°–31° N: A Map Series, *Marine Geophys. Res.* **12**, 247–252.
- Ramberg, I. B., Gray, D. F., and Reynolds, R. G. H., 1977, Tectonic Evolution of the FAMOUS Area of the Mid-Atlantic Ridge, Lat. 35°50' N to 37°20' N, *Geol. Soc. Am. Bull.* **88**, 609–620.
- Ramsay, J. G., 1980, Shear Geometry: A Review, *J. Struct. Geol.* **2**, 1/2, 83–99.
- Rommevaux, C., Deplus, C., and Patriat, P., 1994, Three-Dimensional Study of the Mid-Atlantic Ridge: Evolution of the Segmentation between 28° and 29° N during the Last 10 my, *J. Geophys. Res.* **99**, B2, 3015–3029.
- Rona, P. A., 1976, Asymmetric Fracture Zones and Sea-Floor Spreading, *Earth Planet Sci. Lett.* **30**, 109–116.
- Rona, P. A., Harbinson, R. N., Bassinger, B. G., Scott, R. B., and Nalwalk, A. J., 1976, Tectonic Fabric and Hydrothermal Activity of the Mid-Atlantic Ridge Crest (Lat. 26° N), *Geol. Soc. Am. Bull.* **87**, 661–674.
- Rona, P. A. and Gray, D. F., 1980, Structural Behaviour of Fracture Zones Symmetric and Asymmetric About a Spreading Axis: Mid-Atlantic Ridge (Latitude 23° N to 27° N), *Geol. Soc. Am. Bull.*, part 1, **91**, 485–494.
- Sandwell, D. T. and Smith, W. H. F., 1992, Global Marine Gravity from ERS-1, Geosat, and Seasat Reveals New Tectonic Fabric, *Eos, Trans., Amer. Geophys. Union* **73**, Supplement 43, Fall Meeting, 133.
- Schouten, H., Klitgord, K. D., and Whitehead, J. A., 1985, Segmentation of Mid-Ocean Ridges, *Nature* **317**, 225–229.
- Sclater, J. G. and Francheteau, J., 1970, The Implications of Terrestrial Heat Flow Observations on Current Tectonic and Geochemical Models of the Crust and Upper Mantle of the Earth, *Geophys. J. R. Astr. Soc.* **20**, 509–542.
- Sclater, J. G., Anderson, R. N., and Bell, M. L., 1971, Elevation of Ridges and Evolution of the Central Eastern Pacific, *J. Geophys. Res.* **76**, 7888–7915.

- Searle, R. C., 1986, GLORIA Investigations of Oceanic Fracture Zones: Comparative Study of the Transform Fault Zones, *J. Geol. Soc. Lond.* **143**, 743–756.
- Searle, R. C. and Laughton, A. S., 1977, Sonar Studies of the Mid-Atlantic Ridge and Kurchatov Fracture Zone, *J. Geophys. Res.* **82**, 5313–5328.
- Sempéré, J. C., Purdy, G. M., and Schouten, H., 1990, The Segmentation of the Mid-Atlantic Ridge Between 24° N and 30°40' N, *Nature* **344**, 427–431.
- Sempéré, J. C., Lin, J., Brown, H. S., Schouten, H., and Purdy, G. M., 1993, Segmentation and Morphotectonic Variations Along a Slow-Spreading Center: The Mid-Atlantic Ridge (24°00' N–30°40' N), *Marine Geophys. Res.* **15**, 153–200.
- Severinghaus, J. P. and Macdonald, K. C., 1988, High Inside Corners at Ridge-Transform Intersections, *Marine Geophys. Res.* **9**, 353–367.
- Smith, D. K. and Cann, J. R., 1990, Hundreds of Small Volcanoes on the Median Valley Floor of the Mid-Atlantic Ridge at 24°–30° N, *Nature* **348**, 152–155.
- Smith, D. K. and Cann, J. R., 1992, The Role of Seamount Volcanism in Crustal Construction Along the Mid-Atlantic Ridge at 24°–30° N, *J. Geophys. Res.* **97**, 1645–1658.
- Smith, D. K. and Cann, J. R., 1993, Building the Crust at the Mid-Atlantic Ridge, *Nature* **365**, 707–715.
- Smith, D. K., Cann, J. R., Dougherty, M. E., Lin, J., Spencer, S., Macleod, C., Keeton, J., McAllister, E., Brooks, B., Pascoe, R., and Robertson, W., 1995, Mid-Atlantic Ridge Volcanism From Deep-Towed Side-Scan Sonar Images, 25°–29° N, *J. Volc. Geotherm. Res.* **67** (4), 233–262.
- Tamsett, D. and Searle, R. C., 1988, Structure and Development of the Mid-Ocean Ridge Plate Boundary in the Gulf of Aden: Evidence from GLORIA Side-Scan Sonar, *J. Geophys. Res.* **93**, 3157–3178.
- Tucholke, B. E. and Schouten, H., 1989, Kane Fracture Zone, *Marine Geophys. Res.* **10**, 1–40.
- Tucholke, B. E. and Lin, J., 1994, A Geological Model for the Structure of Ridge Segments in Slow Spreading Ocean Crust, *J. Geophys. Res.* **99**, 11,937–11,958.
- Vogt, P. R., Avery O.E., Schneider E. D., Anderson C. N., and Bracey D. R., 1969, Discontinuities in Sea-Floor Spreading, *Tectonophysics* **8**, 285–317.
- Vogt, P. R., Cande, S., Fox, P. J., and Grindlay, N. R., 1987, Detailed Investigation of a Flow Line Corridor in the South Atlantic: Part 1 – Mid-Atlantic Ridge Crestal Area, *Eos., Trans., Amer. Geophys. Union* **68**, 1491 (Abstract).